array of rods are satisfactory within the limits of the available experimental material. The very small values of q obtained from experiment make the value of its upper limit rather unimportant and it is sufficient that for L of the order of 10^{-3} cm, q is of the order of one. If we put $K'=2$, then the experimental values for L shown in Table II are in good agreement with the theoretical L calculated on the basis of Eq. (27). Consequently the same applies to the calculated values of q and Q_A. The latter are compared with experiment in Fig. 3. Of course the surprisingly good agreement with experiment does not indicate that the specific values assumed for the critical distances between dislocations and between rods or the diameter of the latter are uniquely correct. Rather it indicates that with reasonable values for these quantities the suggested structure of grain boundaries is in accord with experimental observations.

In discussing the intermediate case it was pointed out that the character of the diffusion will depend upon time due to the increasing concentration between the rods. As evident from Eq. (26) and Table I the apparent activation energy will gradually increase with increasing time. However, as experiment shows, this gradual local approach to a uniform grain boundary does not overshadow the basic role of the rod-like structure and the resulting striking variation of Q_A with θ. It is clear that the early idea that a grain boundary varies in a gradual manner from an array of dislocations at small θ to a slab of highly distorted material at high θ, with a gradual decrease of the activation energy from Q_V to Q_B, is in disagreement with experimental data here discussed.

The author wishes to express his appreciation to Dr. F. Adler and Dr. E. G. Olds for help and discussion of some of the mathematical problems.

Note added in proof: C. S. Smith in his discussion to the paper by H. Brooks in the 1951 A.S.M. Seminar on Metal Interfaces points out that the difference between low angle and high angle grain boundaries is easily seen in soap bubble models shown on p. 167 of the above reference. In his paper Brooks indicates schematically, in Fig. 4b, the area of plastic deformation surrounding a dislocation. Formation of a rod would correspond to merging of such areas, of neighboring dislocations, with a concurrent formation of vacancies. The stability of a regular array of such rods is now being investigated. The author is indebted to Dr. F. Seitz for a discussion of these matters.

PHYSICAL REVIEW VOLUME 87, NUMBER 3 AUGUST 1, 1952

Slow Neutron Crystal Spectrometry: The Total Cross Sections of Co, Er, Hf, Ni^{58}, Ni^{60}, Ho, and Fission Sm†

S. BERNSTEIN, L. B. BORST,* C. P. STANFORD, T. E. STEPHENSON, AND J. B. DIAL
Oak Ridge National Laboratory, Oak Ridge, Tennessee

(Received April 11, 1952)

A focusing spectrometer using a variable curvature quartz crystal has been developed for measuring total cross sections *versus* energy of small samples of rare elements, separated isotopes, and radioactive isotopes in the energy region 0.03 ev to about 1.5 ev. Samples having macroscopic cross sections from 0.1 to 1.0 square millimeters have been used as absorbers. The main features of the new instrument are described, and performance curves are given. The instrument was first used to show that a sample of rare earth fission product material has a resonance at an energy corresponding to the known resonance of Sm^{149}. Test runs were made on normal cobalt, whose total cross section was found to fit the formula, σ(barns) $=5.0+6.1(E$ in ev$)^{\frac{1}{2}}$. A resonance at about 1 ev, attributed in the literature to zirconium, was found to belong to hafnium. Erbium was found to have a neutron resonance at about 0.5 ev. Ni^{58} was found to be the isotope primarily responsible for the anomalously high scattering cross section of normal nickel, confirming results from neutron diffraction studies made simultaneously by other observers. Results are given also for Ni^{60}. Analysis of the holmium measurements give a scattering cross section that is strongly energy dependent. Paramagnetic scattering is suggested as a possible explanation of the variation.

I. INTRODUCTION

FOR the past several years we have been interested in the measurement of total cross sections of very small samples of elements rare in the highly pure state and of separated stable isotopes. We have been interested also in the possibility of measuring the cross sections of radioactive isotopes. For these, of course, only microscopic quantities of sample can be made available. In order to achieve acceptable values of transmission the sample and the neutron beam must necessarily be of very small cross-sectional area. Also, because of the intense radiations emitted by the sample, adequate shielding of personnel during the long periods of observation becomes of paramount importance. For this program we have adapted the focusing spectrograph described below, which has been in use for the past several years. This report covers some of the measurements made with it during this period.

† Most of the results reported here in detail were presented briefly at the 288th Meeting of the American Physical Society and appeared in abstract form in the minutes of the meeting, Phys. Rev. **75**, 1302 (1949).

* Now at Department of Physics, University of Utah, Salt Lake City, Utah.

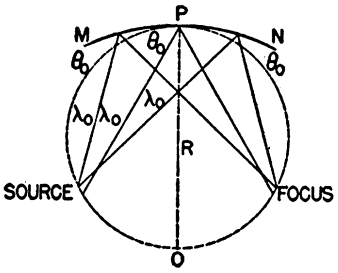

FIG. 1. Approximate focusing spectrograph of Johann.

II. APPARATUS

The focusing spectrometers used in x-ray spectroscopy probably had their origin in the concave grating of Rowland used in optical spectroscopy, in which the source and detector were located on a (Rowland) circle tangent to the grating at its mid-point, the radius of the circle being equal to one-half of the radius of curvature of the grating. For the case of reflection by a crystal, of radiations whose wavelengths are comparable to interatomic distances, where the Bragg law $n\lambda = 2d \sin\theta$ must be satisfied, it is possible, in principle, to construct a perfectly focusing device by bending the crystalline planes to a radius of curvature equal to the diameter of the Rowland circle, and grinding the surface of the crystal to a radius of curvature equal to the radius of the Rowland circle.[1] In many cases in practice, sufficient resolution is procured by using an instrument of the "approximate" focusing type such as those described by Cauchois[2] and by Johann,[2] in which the radii of the crystal surface and of the crystalline planes are equal to the diameter of the Rowland circle. Our instrument corresponds most closely to that of Johann, the arrangement of which is shown in Fig. 1.

In order that the existing concrete shield of the chain reactor could be used in the shielding of radioactive samples, the "point" source was actually in a fixed position four feet inside the outermost face of the pile shield, and so could not be moved along the Rowland circle. The distance from the spectrometer axis of rotation to the detector slit was also fixed. Various energies were selected by first rotating the crystal about an axis through the point P to obtain the appropriate scattering angle. The circle drawn through the source, the axis of rotation of the crystal, and the detector slit determine the radius of the Rowland circle. The radius of curvature of the crystal was then made equal to the diameter of this circle by simply bending it about the point P as a fulcrum, by means of a mechanism that exerted force at the ends M and N of the crystal, until maximum intensity in the detector was attained with a suitable constant size of counter slit width. Radii of curvature required in the energy region in which the instrument was used ran from about 20 feet to 160 feet, so only a very slight bending of the crystal was needed.

A schematic diagram of the arrangement of neutron beam collimator, sample, and detector is shown in Fig 2. The "point" source was procured by means of the long hour-glass-like graphite collimator shown. The beam originates deep inside the pile where the neutron flux is about 10^{12} neutrons per cm^2 per second. The collimator converges uniformly from an initial cross section of 4 inches$\times$4 inches to a diameter of $\frac{3}{8}$ inch at the point S four feet inside the outermost face of the pile shield. A one- or two-mm bore Pyrex capillary tube containing the sample is placed at S so that its axis coincides with that of the collimator. The minimum cross-sectional area of the neutron beam is defined at the sample by the three-inch length of the Pyrex capillary wall. After passing through the sample, the beam diverges again until it strikes the crystal, which focuses it at the detector slit. The crystal is a 5-inch $\times$1-inch$\times$1-mm quartz crystal whose 5-inch$\times$1-inch surface was ground parallel to the 100 planes.

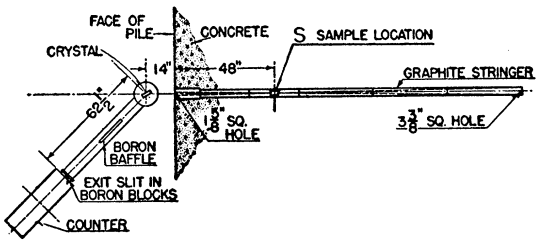

FIG. 2. Schematic arrangement of neutron beam collimator, sample, spectrometer, and detector. The hour-glass like collimator selects those neutrons converging on the sample S, which acts as a "point" source. The beam diverging from the sample is focused by the bent crystal into the detector slit.

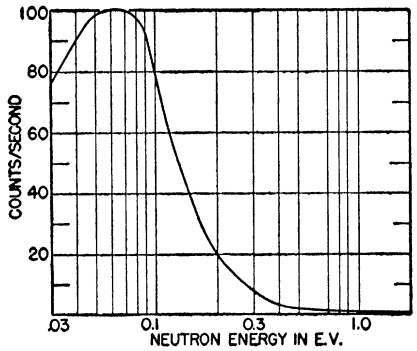

FIG. 3. Counting rate *vs* energy for 2-mm bore capillary tube source and 6-mm detector slit width. Neutron beam from chain reactor is being reflected from 100 planes of quartz crystal.

Actually two identical capillary tubes were used. A very accurately constructed sample shifting device, operated at the pile face, was capable of alternately placing first the sample-containing tube, then an equivalent empty tube, in identically the same position in the neutron beam. The ratio of these two counting rates gives the transmission of the sample.

[1] J. W. Dumond, Rev. Sci. Instr. **18**, 626 (1947).
[2] A. H. Compton and S. K. Allison, *X-Rays in Theory and Experiment* (D. Van Nostrand and Company, Inc., New York, 1935), second edition, pp. 751–753.

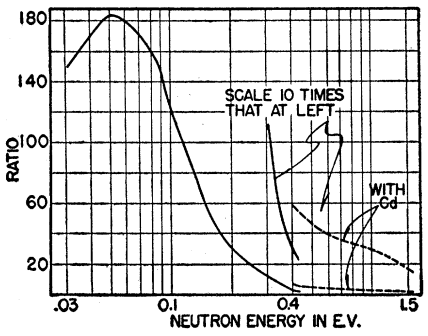

FIG. 4. Ratio of beam count to background count *vs* neutron energy. The scale of ordinates of the three short curves on the right is 10 times the scale of the curve on the left. The curves labeled "with Cd" were taken with a thin foil of Cd over the entrance window of the detector.

The energy spectrum of the neutrons being emitted from the pile is roughly that of a Maxwell distribution corresponding to a temperature of about 540°K. The counting rates as a function of energy actually achieved for a 2-mm bore capillary tube source are shown in Fig. 3. These measured values are due not only to the nature of the incident spectrum, but are affected also by the detector efficiency, crystal reflectivity, solid angle factors, etc. The detector used was a BF_3 proportional counter enriched in the isotope B^{10}. The maximum counting rate was about 6000 counts per minute at about 0.06 ev. The count to background ratio as a function of energy is shown in Fig. 4. It is a maximum of about 180 at 0.05 ev and decreases as the energy increases. The improved ratio above 0.5 ev is obtained by covering the counter slit with a thin foil of cadmium which selectively absorbs the low energy background neutrons because of the neutron resonance of Cd at 0.18 ev.

Figure 5 shows how the counting rate varies at 0.06 ev as the crystal curvature is changed for a 4-mm counter slit width. In addition to improving the energy resolution, the bending of the crystal increases the intensity by about a factor of five. The advantages gained by focusing diminish for the higher energies where the glancing angles become small.

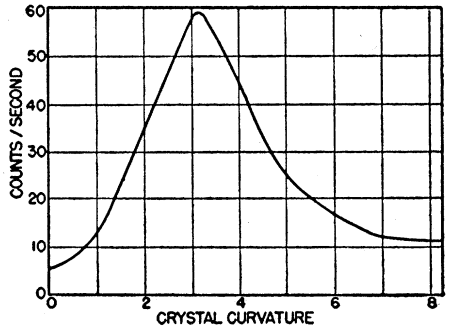

FIG. 5. Counting rate *vs* crystal curvature in arbitrary units at 0.06 ev for a 4-mm counter slit width, illustrating gain in intensity achieved by bending of quartz crystal.

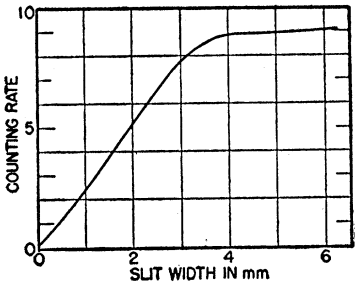

FIG. 6. Counting rate *vs* counter slit width for a 2-mm bore capillary tube source, illustrating focusing properties of spectrometer. For perfect focusing, maximum intensity would be reached for a 2-mm detector slit width.

Figure 6 illustrates the focusing properties of the instrument. It gives counting rate as a function of counter slit width for a 2-mm bore capillary tube source. If the focusing were perfect, the image would also be 2 mm in width. Actually about 90 percent of the maximum counting rate was achieved with a slit width of 3 mm.

The use of crystal diffraction for neutron velocity selection is limited at the lower energies by the presence of higher order reflections. The presence of higher order reflections from the 100 planes of the quartz crystal was studied by transmission measurements of boron as a function of energy. The results plotted in Fig. 7 with the negative of neutron velocity times the logarithm of the transmission as ordinate and energy as abscissa give a straight line parallel to the energy axis, since boron is a $1/v$ absorber. The falling off of the data from this line at energies less than about 0.03 ev is due to the presence of higher order reflections in this region. The lower energy limit of usefulness of the instrument is thus set at about 0.03 ev because of higher order contaminations. The high energy limit of the instrument is set by decreasing beam intensity and increasing background. Measurements are difficult above 0.7 ev.

In order to test the performance of the instrument we measured the cross section of Cd. The peak value of the cross section of Cd at the 0.18-ev resonance agreed within several percent with that of other neutron crystal spectrometer determinations of this quantity.

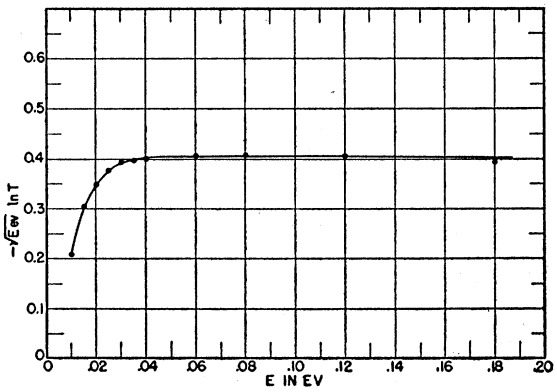

FIG. 7. Absorption of neutron beam reflected from quartz crystal by BF_3 absorber. The falling off from the horizontal line of the points at low energies suggests presence of higher order reflections in beam.

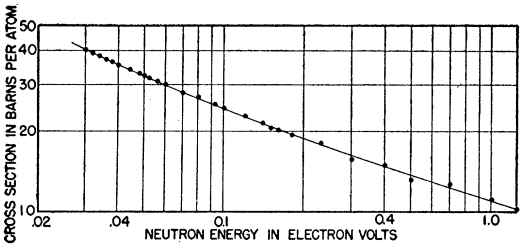

FIG. 8. Transmission cross section of cobalt *vs* neutron energy.

The observed peak value of the cross section is a measure of the resolution of the instrument. The measurements on $Ni^{58}O$, described below, give a very sensitive test of the energy resolution. At 0.028 ev there is a cross-section discontinuity which we carefully investigated. (See Fig. 11.) The energy interval taken to traverse the discontinuity is a measure of the resolution. The measured spread is 0.0006 ev, which corresponds to an effective energy spread of two percent.

III. MEASUREMENTS

The transmission cross section T of a substance is defined by:

$$T=e^{-Nt\sigma_{tr}}, \tag{1}$$

in which (Nt) is the number of scattering or absorbing units per cm^2 in the target material, and σ_{tr} is the total transmission cross section per unit. Expression (1) implicitly assumes that a single event will remove the neutron from the transmitted beam. The total transmission cross section σ_{tr} is the sum of the transmission cross sections for all possible events.

$$\sigma_{tr}=\sum_i \sigma_{tr}^{(i)}, \tag{2}$$

in which $\sigma_{tr}^{(i)}$ may be the transmission cross section for neutron capture, coherent scattering, incoherent scattering due to spin dependence of nuclear forces, incoherent scattering due to presence of isotopes, temperature diffuse scattering, paramagnetic scattering, ferromagnetic scattering in the case of unmagnetized ferromagnetic substances, etc.

The magnitudes of the individual contributions to Eq. (2) depend markedly upon the substance, as the measurements described below illustrate.

A. Neutron Absorption in Rare Earth Fission Products

The first application of the small sample technique was made to evaluate the presence and importance of neutron resonances among the fission products. The existence of large cross-section isotopes among the rare earths implies that at least certain fission product nuclei will have strong neutron absorption.

A sample of uranium metal that had been irradiated one year and had been stored one year after discharge was processed chemically to recover the rare earth fission products from 1.8×10^{20} fissions. The sample, prepared for examination, consisted of 3 mg of dry solid oxalate containing all the rare earth elements, both radioactive and stable.

The sample was mounted in a 1-mm bore Pyrex capillary as the entrance aperture of the curved crystal spectrometer. No attempt was made to shift the sample into and out of the beam. All measurements were taken as total transmission through the sample and compared with measurements made later with a lanthanum oxalate sample of similar size.

The transmission curve showed no evidence of resonance structure except at 0.1 ev. At this energy the transmission dropped to 40 percent and showed a resonance width of 0.03 ev (half-width at half-maximum). Sm^{149} is the only known isotope[3] with a strong resonance at this energy ($E_0=0.096$ ev). Its resonance width, previously measured on this instrument, is 0.035 ev. This value of the absorption corresponds to 7×10^{16} atoms of Sm^{149}. To our knowledge, these results furnished the first evidence that Sm^{149} is a fission product.

Other resonances in the region 0.03 to 0.2 ev would have been observed if as much as 20 percent as intense as the Sm^{149} resonance.

The fission yield of Sm^{149} is reliably reported as 1.3 percent; 2×10^{18} atoms would be expected in the metal before chemical processing, neglecting second-order processes during exposure. Sm^{149}, because of its large capture cross section in the energy region of maximum neutron density, will show strong self-destruction. In the central region of the reactor, Sm^{149} will show a mean life of 120 days. After one year irradiation the correction for self-destruction will be approximately a factor of 5. The calculated amount of Sm^{149} present in the sample examined is therefore 2×10^{17} atoms assuming a chemical yield of 50 percent. The factor of three discrepancy remaining must be considered due to inaccurate knowledge of the conditions of irradiation, chemical yield, and uniformity of the sample.

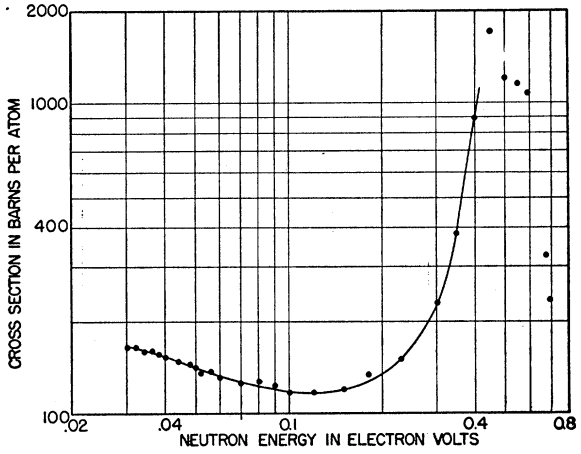

FIG. 9. Transmission cross section of erbium *vs* neutron energy.

[3] Borst, Ulrich, Osborne, and Hasbrouck, Phys. Rev. **70**, 557 (1946).

B. Cobalt

Figure 8 gives the values measured for several samples of cobalt metal between 0.03 ev and 1.2 ev. In this case, if the capture cross section is assumed to vary inversely with velocity, then the sum of all other contributions to the total transmission cross section including the small contribution of ferromagnetic scattering can be taken to be a constant over this energy interval within the accuracy of the observations. The data were fitted by the technique of least squares with the result:

$$\sigma_{tr}=(5.0\pm0.5)+(6.1\pm0.1)E^{-\frac{1}{2}},$$

in which the total cross section σ_{tr} is in barns, and the neutron energy E is in electron volts. The value 38.7 barns is calculated from this expression for the capture cross section at 0.025 ev. Measurements of other observers for this quantity range from 34.2 to 40.5 barns.[4]

C. Erbium

In the case of erbium the sample consisted of 54 mg of Er_2O_3. The results are shown in Fig. 9. A previously unreported resonance was found at about 0.45 ev, whose maximum cross section is about 1700 barns. The data suggest further that perhaps more than one of the isotopes of erbium have a resonance in the region of 0.45 ev and that these resonances overlap.

Europium is known to have a resonance at 0.46 ev.[5] We believe that the observed resonance cannot be accounted for by any europium impurity, since spectroscopic and activation measurements showed that the material contained less than 0.01 percent by weight of other rare earths. This amount of europium impurity could account for less than one barn of the measured cross section at resonance. Extrapolation of the curve from 0.030 to 0.025 ev gives 172 barns as the total cross section. This is to be compared with the value 166±16 barns obtained by the pile oscillator method[4] for the absorption cross section only.

D. Hafnium

Samples of hafnium and zirconium are difficult to obtain in highly pure form because of the similarity in their chemical properties. In addition to the desirability of knowing the neutron cross sections as a function of energy of each of these separately, there was in 1948 an additional point of interest in the neutron absorption properties of these substances because of the fact that the chemical and metallurgical properties of zirconium suggested that it should be very suitable as a reactor structural material. We were especially interested in a resonance that had been reported in the literature for Zr at about 1.1 ev.

We used a quite pure sample of commercially obtained HfO_2. Spectroscopic examination showed 0.7 percent zirconium impurity and less than 0.2 percent

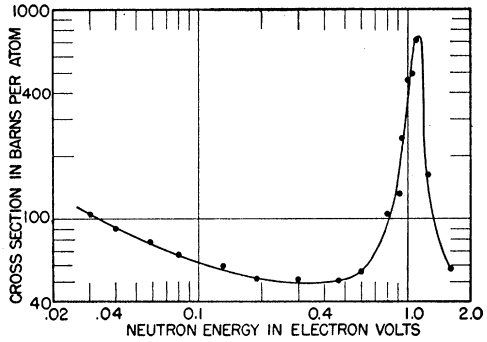

FIG. 10. Transmission cross section of hafnium *vs* neutron energy.

content of other contaminants. Figure 10 shows the results of the measurements. The resonance at 1.1 ev proved to be much stronger than the one reported for zirconium. It was clear then that the resonance belongs to hafnium and that the previously reported resonance at 1.1 ev in zirconium was due to hafnium impurity. Our instrument was not designed for good performance in the region of 1 ev, so that good values for the Breit-Wigner constants of the resonance could not be determined.

Extrapolation of the curve to 0.025 ev gives a total cross section of 115 barns. The data at energies from 0.03 to 0.20 ev were fitted with a constant scattering cross section σ_s, plus a $1/v$ capture cross section. The approximate value of 15 barns was obtained for σ_s. Subtracting 15 barns from the total cross section gives 100 barns as the capture cross section at 0.025 ev, which compares favorably with 102±5 percent obtained by the pile oscillator method[4] but differs considerably from the reported value of 134±8 barns.[6]

E. $Ni^{58}O$

In the case of a crystalline substance consisting of more than one type of scattering center, the transmission cross section per "molecule" for coherent scattering is given by the expression:

$$\sigma_{tr}=\lambda^2 M/2 \sum_{d_{hkl}>\frac{1}{2}\lambda} j_{hkl} d_{hkl} F^2_{hkl} e^{-2W_{hkl}}. \quad (3)$$

λ is the wave length; M is the number of "molecules" per cm^3; j_{hkl} is the multiplicity of the set of planes identified by the Miller indices h, k, l; d is the interplanar spacing; e^{-2W} is a factor that takes into account the zero point and thermal oscillations of the crystal; W is a constant which depends on the Debye temperature and the temperature of the sample; F is the crystal structure factor per molecule. It is given by:

$$F=\sum_{\text{unit cell}} (f_n/N)e^{2\pi i(hx_n+ky_n+lz_n)}, \quad (4)$$

in which N is the number of "molecules" per unit cell; f_n is the coherent scattering amplitude per nth bound nucleus; x_n, y_n, z_n are the coordinates of the nth atom in

[4] H. Pomerance, Phys. Rev. **83**, 641 (1951).
[5] W. J. Sturm, Phys. Rev. **71**, 757 (1947).
[6] P. A. Egelstaff and B. T. Taylor, Nature **167**, 896 (1951).

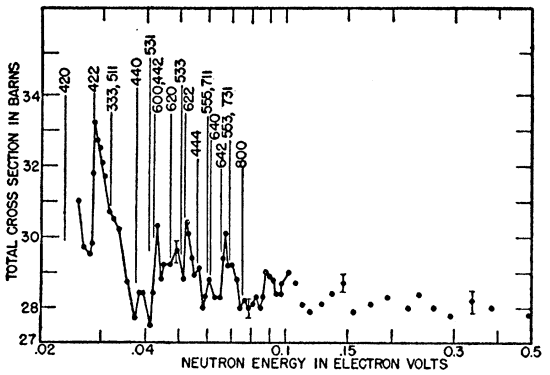

FIG. 11. Transmission cross section of $Ni^{58}O$ *vs* neutron energy.

terms of the primitive lattice translations. The coherent scattering cross section per bound nucleus is $4\pi f_n^2$.

The function defined by Eq. (3) is discontinuous. The contribution to the transmission cross section for coherent scattering of a particular set of planes, *hkl*, increases as λ increases but goes abruptly to zero when the Bragg condition $\lambda = 2d \sin\theta$ cannot be fulfilled, that is, when $\lambda > 2d$. In the case of crystals composed of two types of scatterers for which the scattering amplitudes are not very different, the transmission cross section for coherent scattering is quite sensitive to the relative signs of the amplitudes.

The crystal structure of NiO is the same as NaCl. The unit cell dimension for NiO is $a_0 = 4.172$A. The crystal structure factor per molecule for the various planes are $F = f_{Ni} + f_O$, *h*, *k*, *l*, even; $F = f_{Ni} - f_O$, *h*, *k*, *l*, odd; $F = 0$ for all other reflections.

The measured total cross section per NiO molecule as a function of energy for a sample consisting of 0.148 g of NiO enriched to 98.1 percent in the isotope Ni^{58} is shown in Fig. 11. The Miller indices of the various sets of planes corresponding to the discontinuities are shown. The general pattern of intensities of the various reflections makes necessary the conclusion that the phases of scattering from Ni^{58} and O are the same (positive). This conclusion is especially evident from the fact that the 422 discontinuity is large, the 333, 511 is almost absent, and the 440 is again large.

From the measured height of the 422 discontinuity (5.2×10^{-24} cm^2), using expressions (3) and (4) and the appropriate expression for the crystal structure factor, the coherent scattering amplitude per bound Ni^{58} nucleus, f_{Ni}, has been calculated. In this calculation, the value f_O per bound oxygen nucleus $= 0.58 \times 10^{-12}$ cm[7] has been used; the value of the temperature correction factor e^{-2W} for the 422 reflection was calculated to be $= 0.76$ on the basis of Debye $\theta = 500$°K for NiO. The result $f_{Ni} = 1.5 \times 10^{-12}$ cm per bound Ni^{58} nucleus was obtained, corresponding to a coherent scattering cross section of 27 barns per bound nucleus or 26 barns for the free nucleus. These values agree very well with those of other observers.[7] NiO is known to be antiferromagnetic at room temperature.[8] However, the magnetic structure is such that there will be no contribution to the height of the 422 discontinuity at 0.028 ev.

Since the observed scattering cross section for Ni^{58} is much greater than the potential scattering cross section ($4\pi R^2 \approx 5$ barns), it can be concluded that the scattering at thermal energies is being influenced by the presence of a nearby resonance level of the compound nucleus, and that at thermal energies the resonance scattering and potential scattering interfere constructively.[9]

F. Ni^{60}

The cross section of a 0.219 g sample of NiO enriched to 97.7 percent in the Ni^{60} isotope was measured in the energy range 0.03 to 0.50 ev. The diffraction peaks, though present, were much less pronounced than those for $Ni^{58}O$, corresponding to a much smaller coherent scattering cross section. Since Ni^{58} and Ni^{60} together account for 94 percent of the abundance of normal nickel, the cross-section measurements for these two separated isotopes show that Ni^{58} is the isotope responsible for the anamolously high scattering cross section of normal nickel. Our sample contained 1 percent water impurity, for which corrections were made. When subtractions were made also for the scattering by the oxygen and for the capture by the Ni^{60} ($\sigma_c = 2.70$b at 0.025 ev)[10] the resulting scattering cross section for Ni^{60} was much less than $4\pi R^2 \approx 5$ barns, suggesting a scattering resonance at an energy such that the resonance scattering and the potential scattering interfere destructively. This low value of the scattering cross section of Ni^{60} is consistent with the results of other observers.[7]

G. Holmium

The material was used in the form of the oxide Ho_2O_3. It was separated from other rare earths by means of the ion-exchange-column technique. Spectroscopic and activation measurements proved that there was less than 0.1 percent of all other rare earths present. Two anhydrous samples were prepared, 0.042 and 0.0668 g.

The total cross section of the oxygen[11] in the molecule was subtracted from the observed values. The total cross section per holmium atom (σ_{tr}) from 0.026 ev to 0.5 ev is given in Fig. 12. Small irregularities due to coherent nuclear scattering appear in the data. Individual discontinuities due to the contributions of some one set of planes could not be resolved because of the small heights of the irregularity and the large number of different sets of planes contributing in the small energy region where the irregularities appeared. Several values[12,13,4] reported in the literature for the thermal

[7] C. G. Shull and E. O. Wollan, Phys. Rev. **81**, 527 (1951).

[8] Shull, Strauser, and Wollan, Phys. Rev. **83**, 333 (1951).

[9] Feshbach, Peaslee, and Weisskopf, Phys. Rev. **71**, 145 (1947).

[10] H. Pomerance (unpublished).

[11] Goldsmith, Ibser, and Feld, Revs. Modern Phys. **19**, 259 (1947).

[12] W. Bothe, Z. Naturforsch. **1**, 179 (1946).

[13] Seren, Friedlander, and Turkel, Phys. Rev. **72**, 888 (1947).

neutron capture cross section of holmium are 49, 59.6, and 64 barns. The first two of these values were obtained by the activation technique, while the latter result was obtained with the pile oscillator. In interpreting our data we have used the 64-barn value for the absorption cross section since the material used in the measurement of this value and the material used in our measurements came from the same batch of purified holmium. The value 64 barns corresponds to an average neutron energy of 0.025 ev.

The dependence of the value of the capture cross section of holmium (σ_c) on energy is not known. If the assumption is made that it varies as $1/v$, then the scattering cross section $\sigma_s=\sigma_{tr}-\sigma_c$ decreases from 31 barns at 0.025 ev to 14 barns at 0.5 ev. Since the Ho^{+++} ion possesses an effective magnetic moment of 10.5 Bohr magnetons, this variation of scattering cross section with energy may possibly be due to paramagnetic scattering. The observation of paramagnetic scattering in measurements of total cross section has previously been reported.[14] We have calculated from our data a paramagnetic scattering cross section (σ_{pm}), per Ho^{+++} ion as a function of energy. The resulting points are shown in Fig. 12. They result from the equation $\sigma_{tr}=\sigma_c+\sigma_s+\sigma_{pm}$ and the following assumptions: (a) the capture cross section of holmium, σ_c, varies inversely as the velocity; (b) the transmission cross section due to scattering other than paramagnetic scattering is approximately constant over the energy region of our measurements. The total cross-section data show that the irregularities due to coherent nuclear scattering are small.

The lower curve of Fig. 12 is the paramagnetic cross section *vs* energy, calculated from the following expression:[15]

$$\sigma_{pm}=\tfrac{2}{3}\pi(e^2\gamma/mc^2)^2 g_J^2 J(J+1)F, \qquad (5)$$

in which the symblls e, m, and c have their usual significance; γ is the neutron magnetic moment in nuclear Bohr magnetons; and g_J is the gyromagnetic ratio of the normal state, $^5J_8$ of the Ho^{+++} ion. It was computed from the landé g formula for Russell-Saunders coupling. F is the average over-all scattering angles of the square of the atomic scattering factor of the $4f$ shell. The semi-empirical atomic scattering factors[16] of Pauling and Sherman were used to obtain F. In Eq. (5) we have replaced the usual $g_S^2S(S+1)$, for cases in which the orbital angular momentum is quenched with $g_J^2J(J+1)$, since the value of the effective magnetic moment (μ) of the Ho^{+++} ion as determined from magnetic susceptibility measurements agrees very well with the value calculated by setting $\mu=g_J[J(J+1)]^{\frac{1}{2}}$.[17] The paramagnetic cross section deduced from the data and that calculated using Eq. (5) have been set equal to each other at 0.5 ev. Normalization at 0.5 ev exhibits the increasing deviation between observed and calculated values as the energy decreases.

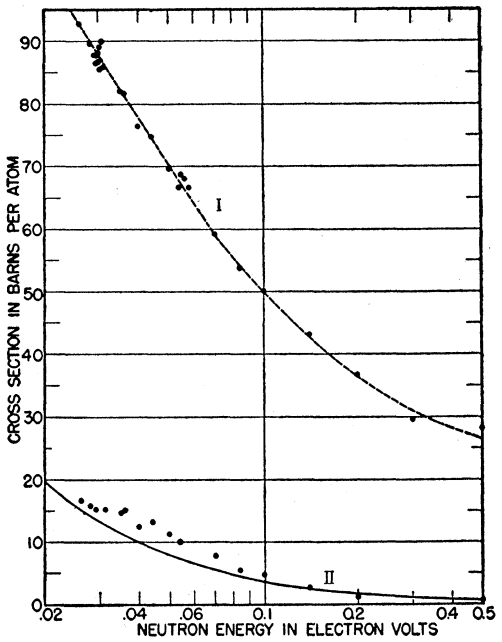

FIG. 12. Cross section of holmium *vs* energy. The points along curve I are the measured total cross sections. Curve I is drawn through the average of these points, smoothing out any small irregularities which may be due to coherent scattering. Curve II is the calculated paramagnetic scattering cross section. The points along curve II are deduced from curve I by subtracting capture and nuclear scattering.

The data agree roughly with the calculated curve in shape and absolute value. In view of the assumptions made, further discussion of the quality of the agreement between "observed" and calculated paramagnetic cross section seems hardly justifiable. The existence of a nuclear resonance at an energy lower but not distant from the lowest energy at which measurements were taken could completely alter the interpretation. Additional measurements of the total cross section at energies greater than 0.5 ev and in the region of low energies where there is no coherent scattering would also be helpful.

ACKNOWLEDGMENT

We are grateful to many of our colleagues at Oak Ridge National Laboratory for their assistance in carrying out the work described in this report. The sample of rare earth fission products was prepared by Dr. P. Thompkins and Dr. R. Overman. Dr. G. Boyd and Mr. D. Harris prepared the pure samples of rare earths. The separated nickel isotopes were prepared under the direction of Dr. C. P. Keim. Mr. D. E. LaValle performed the analyses of our samples for water content. Miss T. Arnette assisted in taking much of the data. We are grateful to Dr. E. O. Wollan and Dr. C. G. Shull for many helpful discussions.

[14] I. W. Ruderman, Phys. Rev. **76**, 1572 (1949).
[15] O. Halpern and M. H. Johnson, Phys. Rev. **55**, 898 (1939).
[16] L. Pauling and J. Sherman, Z. Krist. **81**, 1 (1932).
[17] L. F. Bates, *Modern Magnetism* (Cambridge University Press, Cambridge, 1948), p. 127.